Eur J Cancer, Vol. 27, No. 12, pp. 1560–1564, 1991.
Printed in Great Britain

0277–5379/91 $3.00 + 0.00

A Prospective Comparison between Magnetic Resonance Imaging, Meta-iodobenzylguanidine Scintigraphy and Marrow Histology/Cytology in Neuroblastoma

Robin Corbett, Julie Olliff, Neil Fairley, Judy Moyes, Janet Husband, Ross Pinkerton, Richard Carter, Jennifer Treleaven, Timothy McElwain and Simon Meller

A prospective comparison between magnetic resonance imaging (MRI), ^{123}I meta-iodobenzylguanidine (mIBG) scintigraphy and posterior iliac crest marrow aspiration and trephine biopsy in 30 assessments (19 patients) showed concordance between the three techniques in 16 assessments (53.3%). In 10 (33.3%), MRI and mIBG revealed abnormalities not detected by marrow biopsy. MRI was the only technique to demonstrate marrow abnormality in four assessments (13.3%). In addition, MRI revealed more sites of abnormality in 16 parallel assessments. We conclude that MRI shows promise as a non-invasive means of detecting bone marrow infiltration by neuroblastoma, but that further evaluation of the specificity of MRI in this setting is indicated.
Eur J Cancer, Vol. 27, No. 12, pp. 1560–1564, 1991.

INTRODUCTION

NEUROBLASTOMA IS the most common extracranial solid tumour of childhood. Primary tumours most often arise in the adrenal medulla or paravertebral sympathetic chain; however, at diagnosis the majority of neuroblastomas have metastasised to distant sites, most commonly the bone marrow [1]. Metastatic neuroblastoma is initially treated with intensive combination chemotherapy, following which the disease is reassessed. In our unit, if the bone marrow is clear, surgery to remove the primary tumour is followed by high-dose chemotherapy and autologous bone marrow transplantation (ABMT) [2]. Despite this aggressive approach, two thirds of patients relapse implying the presence of undetected residual disease at the time of reassessment. The conventional method for assessing the bone marrow in neuroblastoma is cytological and histological examination of marrow removed from both posterior iliac crests [3]. However, marrow involvement by neuroblastoma is typically patchy, inevitably resulting in some false negative results if the iliac crests are the only sites of examination [4].

There are potential benefits of more accurate marrow evaluation. More sensitive techniques employed at the time of diagnosis may identify patients with small volume metastatic disease who would be understaged using conventional methods; these patients may benefit from more intensive therapy. At reassessment, residual metastatic marrow disease, following intensive chemotherapy, is likely to imply the need for further consolidation treatment. In addition, these patients may benefit from purging of their marrow (i.e. *in vitro* removal of residual tumour cells by immunological techniques or cytotoxic drugs) prior to ABMT.

In recent years meta-iodobenzylguanidine (mIBG) scintigraphy has been increasingly employed to identify neuroblastoma [5]. It is used in the diagnosis, staging and reassessment of patients with neuroblastoma, and has been shown to be highly sensitive and specific in this condition [6]. Magnetic resonance imaging (MRI) is extremely sensitive in detecting abnormalities of bone marrow [7, 8]. Couanet and Geoffray (1988) have described the typical MR appearances of bone marrow infiltration by neuroblastoma [9].

This study was undertaken prospectively to compare the results of MRI, mIBG scintigraphy, and cytological and histological examination of posterior iliac crest marrow, in the detection of marrow infiltration by neuroblastoma.

PATIENTS AND METHODS

Patients

The clinical details of the 19 patients studied are documented in Table 1. 10 girls and 9 boys with a median age of 4 years 9 months at diagnosis (range of 6 months to 13 years 7 months) were investigated. A diagnosis of neuroblastoma was established in all patients, according to the International Neuroblastoma Staging System (INSS) criteria [1]. 3 had stage 3 disease (INSS classification) (patients 16, 17 and 19) and the remaining 16 patients had stage 4 disease (of the latter group, only patient 4 did not have marrow infiltration at diagnosis).

Approval to undertake the study was obtained from the hospital ethics committee.

MRI

MRI was performed on a Siemens Magneton machine operating at 1.5 Tesla. T1 weighted (TR 500 ms, TE 17 ms) spin-echo sagittal images were obtained of the thoraco-lumbar spine along with T1 weighted (TR 500 ms, TE 17 ms) spin-echo coronal images of the pelvis and femora. In addition, T2 weighted images (TR 2100 ms, TE 70/90 ms) were obtained on

Correspondence to R. Corbett.
R. Corbett, J. Moyes, R. Pinkerton, T. McElwain and S. Meller are at the Department of Paediatrics; J. Olliff, N. Fairley and J. Husband are at the Department of Radiology; R. Carter is at the Department of Histopathology; and J. Treleaven is at the Department of Haematology, Royal Marsden Hospital and Institute of Cancer Research, Downs Road, Sutton, Surrey SM2 5PT, U.K.
Revised 5 Aug. 1991; accepted 22 Aug. 1991.

Table 1. Clinical details of patients studied

Patient/sex	Age at diagnosis (yr:mo)	Assessment no.	Treatment before assessment
1/F	3	1	OPEC, Surgery
2/F	0:6	1	OPEC, HDM (relapse)
		2	Carboplatin
		3	Carboplatin
3/M	4:9	1	Untreated
		2	OPEC, Surgery
		3	mIBG, HDM, carboplatin
4/F	9:6	1	OPEC
		2	mIBG, OMEC
5/M	3:10	1	OPEC, Surgery
6/M	8	1	OPEC
		2	Surgery, carboplatin
7/M	8:9	1	OPEC, Surgery
8/M	4:4	1	OPEC, Surgery
		2	no further treatment
9/M	1:9	1	OPEC, Surgery
10/F	7	1	OPEC
		2	mIBG
		3	Carboplatin
		4	No further therapy
11/F	4:6	1	OPEC
12/F	3:4	1	OPEC
		2	mIBG
13/F	9:4	1	OPEC, Surgery, carboplatin
14/F	13:7	1	O,P,C,dox,ifos,pepti,surgery
15/M	2:6	1	No treatment (relapse)
16/M	5	1	Carboplatin, RT (relapse)
17/F	12:6	1	Untreated
18/F	2:6	1	Untreated
19/M	5:6	1	No treatment (relapse)

OPEC = alternating cycles of vincristine, cisplatin, etoposide and cyclophosphamide; HDM = high-dose melphalan with autologous bone marrow rescue (ABMT); OMEC = high-dose vincristine, melphalan, etoposide and carboplatin, followed by ABMT; mIBG = ^{131}I meta-iodobenzylguanidine therapy; O = vincristine; P = cisplatin; C = cyclosphosphamide; dox = doxorubicin; ifos = ifosfamide; pepti = peptichemio [10]; RT = local radiotherapy to tumour.

8 patients whose T1 weighted scans showed focal marrow abnormalities. Potentially uncooperative patients were sedated before the examination which took 40–60 minutes to complete; older patients were scanned over two sessions. The T2 weighted images on patient 16 were degraded by motion artefact, otherwise the examinations were well tolerated.

mIBG scintigraphy

The thyroid gland was blocked with potassium iodide. 24 h after the intravenous administration of 185 MBq ^{123}I mIBG (Amersham, Germany), patients were scanned using a General Electric Starcam camera with dedicated computer and a high-resolution, low-energy, parallel hole collimator. Six to eight anterior and posterior images were acquired, each over 10 min ($4–5 \times 10^5$ counts per image), to provide a composite whole body scan. Films were examined by three paediatricians with a particular interest in mIBG scintigraphy (RC, JSEM and STM). Scintillation above background in regions conforming to bone marrow compartments was interpreted as a positive mIBG scan.

Bone marrow examination

A standardised procedure for bone marrow biopsy and study was adopted for all patients. Bone marrow was aspirated and trephine biopsies performed from the right and left posterior iliac crests. Tissues for histology were fixed in 10% formyl-saline, resin-embedded, cut at 1.5 μm and stained routinely with haematoxylin and eosin, and with Giemsa. Cytological assessment of bone marrow was performed by examination of spread films of aspirated material stained with May–Grunwald–Giemsa.

Evaluation of positive sites on MRI and mIBG scans

In order to determine whether MR or mIBG imaging revealed a greater number of abnormalities, films were scored according to the presence or absence of abnormalities in ten locations within the bone marrow compartment—thoracic and lumbar vertebral bodies, pelvis (left and right), and the upper, mid and lower shaft of each femur. Each of the three examinations was reported independently without knowledge of the other results.

RESULTS

Thirty parallel assessments were performed on 19 patients. Three assessments were performed at diagnosis (patients 3, 17 and 18), four at relapse (patients 2, 15, 16 and 19), and the remainder during or after initial therapy. In all except one study, the three investigations were performed within a 2-week period. Six weeks after MRI and mIBG scanning, marrow examination was carried out on patient 8. This patient received no anticancer therapy during this interval and the marrow examination was negative. Inadequate trephine biopsies were obtained from 2 patients (nos 3 and 4, both assessment 1) whose standard posterior iliac crest marrow examination consisted of cytological assessment alone. In all other assessments, the quality of the histological and cytological specimens was deemed to be satisfactory.

Table 2 shows the comparison of results of MRI, mIBG and marrow cytology/histology. Groups A and D are those in which there was concordance between the three techniques; groups B and C represent the studies in which discordance was noted. There was overall agreement in 16/30 assessments (53.3%) (Groups A and D).

Group C represents 3 patients (4 assessments) in whom MRI was the only investigation to reveal abnormality (13.3% of assessments). On two occasions, MRI alone demonstrated an abnormality in the body of L3 in patient 4. This region was abnormal on a ^{99m}technetium MDP bone scan, but uptake of mIBG into a large abdominal tumour probably prevented visualisation of this lesion on the planar scintigram. MRI was the sole modality to reveal bone marrow abnormalities (in the upper femora and pelvis) in patient 7, the focal areas of abnormal signal all measuring less than 1.5 cm in diameter. This patient

Table 2. Comparison of results of MRI, mIBG and marrow cytology/histology

Group	MRI	mIBG	Cytology/ Histology	No. of examinations
A	+	+	+	13 (43.3%)
B	+	+	−	10 (33.3%)
C	+	−	−	4 (13.3%)
D	−	−	−	3 (10.0%)

died shortly after the assessment as a result of toxicity due to OMEC chemotherapy, and confirmation of the nature of the MRI abnormalities was not obtained. Patient 16 died of progressive disease 5 months after MRI alone showed an abnormality in a lower thoracic vertebral body.

In 7 patients (10 assessments) both MRI and mIBG scans were positive and marrow examinations negative (Group B). In 2 of these patients (8 and 15) direct aspiration of marrow from areas of abnormality revealed cytological evidence of infiltration by neuroblastoma (Figs 1a, b). Furthermore, patients 6, 10, 11 and 12 had positive marrow examinations 6 weeks to 7 months after the assessments in which only mIBG and MRI demonstrated marrow abnormality. The second and third assessments in patient 3 revealed a distinct area of high signal on the T2 weighted images in the right upper femur; this patient subsequently developed a limp and complained of pain in the right hip. A plain X-ray revealed a lytic lesion at this site. This patient died of progressive disease 9 months after the third assessment.

12 patients (group 1) were examined on a single occasion, whilst the remaining 7 patients underwent a total of 18 assessments (group 2). MRI was positive in all group 2 assessments, but negative in 3 group 1 assessments. In 2 patients from group 1 and 1 from group 2 (who had 2 assessments) MRI was the only positive investigation.

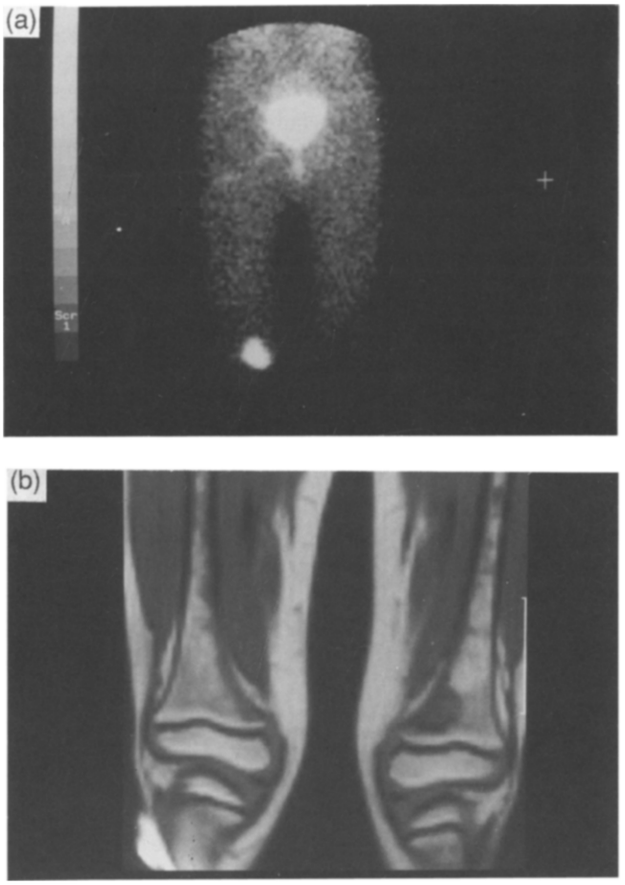

Fig. 1. (a) Posterior ^{123}I mIBG scintigram showing abnormal isotope uptake in the medial aspect of the left femur (patient 8, assessment 1). (b) The T1-weighted (TR 500 ms, TE 17 ms) coronal MR scan showing an abnormal area of low marrow signal corresponding to the area of high isotope uptake. An aspirate from the distal femoral lesion demonstrated viable neuroblastoma (patient 8, assessment 1).

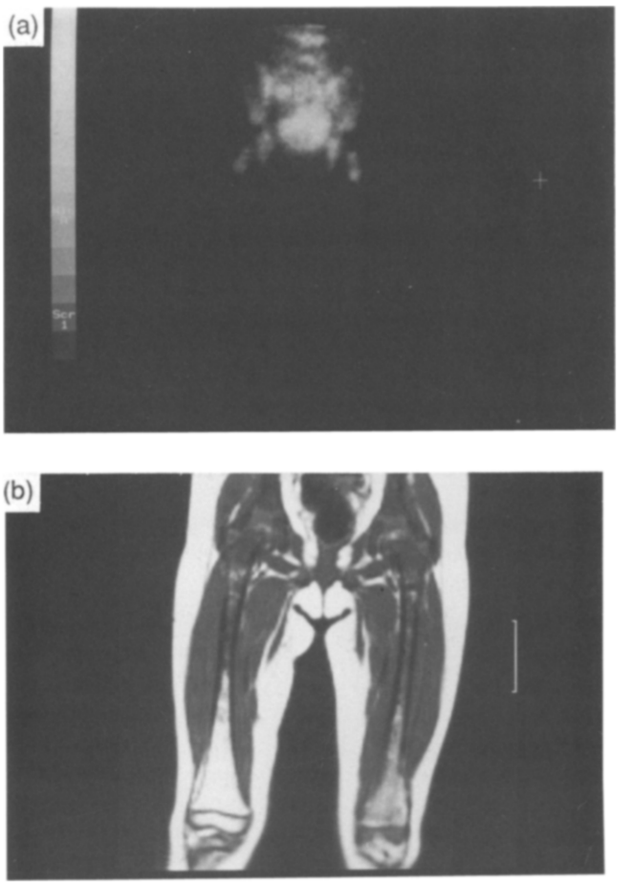

Fig. 2. (a) Posterior ^{123}I mIBG scintigram showing abnormal isotope uptake in the lower lumbar spine, pelvis and proximal femoral shafts (patient 2, assessment 1). (b) Coronal T1-weighted (TR 500 ms, TE 17 ms) MR scan showing abnormal signal in the proximal two-thirds of the right femoral shaft and throughout the left femur. In comparison with the mIBG scan, MR shows a greater extent of marrow abnormality in the femora (patient 2, assessment 1).

In 77% of the assessments (23/30), both MRI and mIBG were positive (Groups A and B, Table 2). These scans were analysed according to the number of sites of abnormality revealed by the individual imaging techniques. In 7/23 assessments MRI and mIBG scans demonstrated the same extent of abnormality. In the remaining 16 studies on 10 patients, MRI revealed a median of four more sites of abnormality per scan (range 1–9) than mIBG scintigraphy. These additional sites of abnormality were noted in the femora only in nine assessments, and in the femora, pelvis and vertebral bodies in seven assessments (Figs 2a, b). Thirteen anatomical sites (10 assessments on 8 patients) with decreased T1 weighted signal intensity were studied using T2 weighting. In 7 sites the T2 signal was increased, and in 5 of these the corresponding mIBG scan was positive. In 4/6 sites in which the T2 weighted signal intensity was either normal or decreased, the mIBG scan was positive at the corresponding site.

DISCUSSION

The most common cytological pattern of infiltration by neuroblastoma is random clumping of neuroblasts amongst the haemopoietic elements. Histologically, tumour cells in the bone marrow are often scanty and the characteristic architecture with rosettes is rarely seen [11]. It is not surprising that false negative

posterior iliac crest marrow examinations are encountered. This study was undertaken to test the hypothesis that non-invasive imaging techniques would be more suited to detecting multifocal marrow deposits, because they are able to examine a larger marrow volume than morphological examination of samples from the posterior iliac crests.

In 14/30 assessments (47%), either MRI alone (group C, Table 2) or MRI and mIBG (group B) were positive, but standard marrow examination negative. However, a number of techniques not employed in this study may improve the detection of marrow infiltration by neuroblastoma. Changes in the normal marrow architecture, such as fibrosis, may indicate malignant infiltration in the absence of direct demonstration of malignant cells [12]. Monoclonal antibodies (e.g. UJ13A and anti-GD2) significantly increase the sensitivity of iliac crest marrow examination [4, 13, 14]. Immunocytology was performed in a minority of assessments in our study; results were therefore not included in the analysis.

Improved tumour detection may be achieved by examining marrow aspirated from 10 sites (eight from the pelvis and two from the sternum) [15]. Despite this aggressive approach, mIBG scans showing marrow infiltration have been encountered in patients with negative multiple aspirates [16]. Feine *et al.* [6] have reported >90% sensitivity and specificity of mIBG scintigraphy in assessing neuroblastoma at diagnosis. However, lesions may not be detected on planar scans when they are obscured by overlying areas of activity (this probably explains the negative mIBG marrow assessment in patient 4). Single photon emission computed tomography (SPECT) separates overlapping regions of uptake; ^{123}I mIBG SPECT permits detection of more lesions than planar scintigraphy alone but was not employed in our study [17]. After intensive chemotherapy, sensitivity of planar mIBG scintigraphy decreases to approximately 70% [6], probably due to the adverse effect of chemotherapy on the active uptake mechanism [18]. Thus, a technique for assessing the bone marrow compartment, other than mIBG scanning or standard iliac crest biopsy, is desirable.

For MRI, the major determinant of contrast resolution in bone marrow is fat which produces a short T_1 and relatively longer T_2 relaxation time. In childhood, almost the entire medullary cavity contains red marrow (consisting of 25–50% fat cells); the T_1 signal is lower than that for yellow marrow, and T_2 signal may be of higher intensity [7]. Diseases that infiltrate bone marrow displace fat cells and consistently produce a prolongation of the T_1 relaxation time [19, 20]. In our study there was poor correlation between positive mIBG marrow scans and hyperintense signal on T_2 weighted scans in keeping with studies which have reported widely variable signal intensity on T_2 weighted images of malignant marrow infiltration [21, 22]. These results suggest that T_1 weighted spin-echo sequences are likely to be more sensitive in demonstrating marrow infiltration than T_2 weighted scans.

Eighteen of 30 assessments (67%) were performed on 7 patients who had more than 1 assessment. It is inherent in this type of study that bias may be introduced by examining patients on more than one occasion, but we believe this does not detract from the overall conclusions drawn from the analysis. Our study shows that MRI is more sensitive than mIBG scintigraphy or standard iliac crest marrow examination in revealing the presence and extent of marrow abnormality in children with neuroblastoma. However, only in a minority of cases was the actual area of MRI abnormality biopsied, leaving the issue of specificity largely unanswered.

In a similar study of 5 patients with neuroblastoma, MRI was more sensitive than scintigraphy using ^{131}I-3F8 (a monoclonal antibody against GD2 antigen) in detecting marrow abnormality, but the specificity of MRI was not confirmed [23].

At diagnosis, the presence of low signal areas in bone marrow on T_1 weighted images would be very suggestive of marrow metastases. However, non-malignant conditions such as infection and infarction produce a similar appearance. Islands of residual red marrow seen during physiological red to yellow marrow conversion [7] could confuse interpretation in an adolescent (only 2 assessments were performed on patients older than 12 years in our study). At reassessment after chemotherapy, irradiation or bone marrow transplantation the issue of specificity becomes less clear. Following therapy, acute changes in the marrow, such as oedema, inflammation and necrosis produce a low signal on T_1 weighted images, and a high T_2 weighted image signal [24]. Subsequent myelofibrosis, fatty infiltration and haemopoeitic reconstitution may further confuse interpretation [25]. 90% (27/30) of assessments in our study were performed after treatment; acute and chronic reactions of bone marrow to therapy may have produced spin-echo signal intensities simulating malignant infiltration on some scans. However, the sensitivity and specificity of MRI in detecting malignant infiltration may be enhanced by techniques not used in our study, such as alternative pulse sequences e.g. STIR, proton chemical shift imaging and MR spectroscopy [24, 26–29].

MRI of the bone marrow, in an attempt to detect marrow metastases, is time-consuming and costly. At present, routine use of MRI in this role is not to be encouraged. It is recommended that patients with marrow abnormalities detected by MRI alone undergo biopsy to determine the histological nature of the abnormality; such a study is underway at our hospital.

1. Brodeur GM, Seeger RC, Barrett A, *et al.* International criteria for diagnosis, staging and response to treatment in patients with neuroblastomas. *J Clin Oncol* 1988, **6**, 1874–1881.
2. Pinkerton CR, Pritchard J, de Kraker J, Jones D, Germonds S, Love S. ENSG I—randomized study of high dose melphalan in neuroblastoma. In: KA Dicke, G Spitzer, S Jagannath, eds. *Autologous Bone Marrow Transplantation*. University of Texas Press, Houston, 1987, 401–405.
3. Franklin IM, Pritchard J. Detection of bone marrow invasion by neuroblastoma is improved by sampling at two sites with both aspirates and trephine biopsies. *J Clin Pathol* 1983, **36**, 1215–1218.
4. Favrot MC, Frappaz D, Maritaz O, *et al.* Histological, cytological and immunological analyses are complementary for the detection of neuroblastoma cells in bone marrow. *Br J Cancer* 1986, **54**, 637–641.
5. Moyes J, McCready VR, Fullbrook A. *Neuroblastoma. MIBG in its Diagnosis and Management*. Berlin, Springer, 1989.
6. Feine U, Muller-Schauenburg W, Treuner J, Klingebiel T. Metaiodobenzylguanidine (mIBG) labeled with ^{123}I/^{131}I in neuroblastoma diagnosis and follow-up treatment with a review of the diagnostic results of the International Workshop of Paediatric Oncology held in Rome, September 1986. *Med Pediatr Oncol* 1987, **15**, 181–187.
7. Vogler JB, Murphy WA. Bone marrow imaging. *Radiology* 1988, **168**, 679–693.
8. Cohen MD, Klatte EC, Baehner R, *et al.* Magnetic resonance imaging of bone marrow disease in children. *Radiology* 1984, **151**, 715–718.
9. Couanet D, Geoffray A. Etude en imagerie par resonance magnetique (IRM) des metastases osteomedullares des neuroblastomes. *Bull Cancer* 1988, **75**, 91–96.
10. De Bernadi B, Pastore G, Carli M, *et al.* Effect of peptichemio in nonlocalized neuroblastoma. *Cancer* 1982, **50**, 10–17.
11. Mills AE, Bird AR. Bone marrow changes in neuroblastoma. *Pediatr Pathol* 1986, **5**, 225–234.
12. Reid MM, Hamilton PJ. Histology of neuroblastoma involving bone

marrow: the problem of detecting residual tumour after initiation of chemotherapy. *Br J Haematol* 1988, **69**, 487–490.
13. Rogers DW, Treleaven JG, Kemshead JT, Pritchard J. Monoclonal antibodies for detecting bone marrow invasion by neuroblastoma. *J Clin Pathol* 1989, **42**, 422–426.
14. Cheung NV, von Hoff DD, Strandjord SE, Coccia PF. Detection of neuroblastoma cells in bone marrow using GD2 specific monoclonal antibodies. *J Clin Oncol* 1986, **4**, 363–369.
15. Bayle C, Allard T, Rodary C, Vanderplancke J, Hartmann O, Lemerle J. Detection of bone marrow involvement by neuroblastoma: comparison of two cytological methods. *Eur J Pediatr Haematol Oncol* 1985, **2**, 123–128.
16. Lumbroso JD, Guermazi F, Hartmann O, *et al.* Meta-iodobenzylguanidine (mIBG) scans in neuroblastoma sensitivity and specificity, review of 115 scans, In: Evans AE, D'Angio GJ, Seeger RC, eds. *Advances in Neuroblastoma Research*. New York, Liss, 1988, 689–705.
17. Corbett R, Fullbrook A, Meller ST. ^{123}I metaiodobenzylguanidine (mIBG) SPECT in the assessment of children with neuroblastoma. *Prog Clin Biol Res* 1991, **366**, 479–486.
18. Paffenholz V, Ebener U, Kornhuber B. Uptake and release of iodine-labelled m-iodobenzylguanidine in a neuroblastoma cell culture system and its importance in neuroblastoma therapy. *J Cancer Res Clin Oncol* 1989, **115**, 269–275.
19. Moore SG, Gooding CA, Brasch RC, *et al.* Bone marrow in children with acute lymphoblastic leukaemia: MR relaxation times. *Radiology* 1986, **160**, 237–240.
20. Smith SR, Williams CE, Davies JM, Edwards RHT. Bone marrow disorders characterization with quantitative MR imaging. *Radiology* 1989, **172**, 805–810.
21. Porter BA, Shields AF, Olson DA. Magnetic resonance imaging of bone marrow disorders. *Radiol Clin N Am* 1986, **24**, 269–289.
22. Dietrich RB, Kangarloo H, Lenarsky C, Feig SA. Neuroblastoma: the role of MR imaging. *Am J Radiol* 1987, **148**, 937–942.
23. Fletcher BD, Miraldi FD, Cheung NV. Comparison of radiolabeled monoclonal antibody and magnetic resonance imaging in the detection of metastatic neuroblastoma in bone marrow: preliminary results. *Pediatr Radiol* 1989, **20**, 72–75.
24. McKinstry CS, Steiner RE, Young AT, Jones L, Swirsky D, Aber V. Bone marrow in leukaemia and aplastic anaemia: MR imagining before, during, and after treatment. *Radiology* 1987, **162**, 701–707.
25. Lanir A, Aghai E, Simon JS. MR imaging in myelofibrosis. *J Comput Assist Tomogr* 1986, **10**, 634–636.
26. Bydder GM, Young IR. MR imaging: clinical use of the inversion recovery sequence. *J Comput Assist Tomogr* 1985, **9**, 659–675.
27. Pykett FL, Rosen BR. Nuclear magnetic resonance: *in vivo* proton chemical shift imaging. *Radiology* 1983, **149**, 197–201.
28. Rosen BR, Fleming DM, Kushner DC *et al.* Haematologic bone marrow disorders: quantitative chemical shift MR imaging. *Radiology* 1988, **169**, 799–804.
29. Aisen AM, Chenevest TL. MR spectroscopy: clinical perspective. *Radiology* 1989, **173**, 593–599.

Acknowledgements—R.C. is supported by the Royal Marsden Hospital Clinical Research Fund. MRI research is funded by the Cancer Research Campaign.

Eur J Cancer, Vol. 27, No. 12, pp. 1564–1566, 1991.
Printed in Great Britain

0277–5379/91 $3.00 + 0.00

Synchronous Cisplatin Infusion During Radiotherapy for the Treatment of Metastatic Melanoma

Mark A. Rosenthal, Colin A. Bull, Alan S. Coates, Graham Stevens, W.H. McCarthy, H. Mameghan and Richard F. Kefford

In two pilot studies, 55 patients with symptomatic metastases from malignant melanoma were treated with irradiation and concurrent cisplatin. In the first group, cisplatin was given as a continuous intravenous infusion of 20 mg/m^2 per day on days 1–5 and 22–26, with irradiation on days 2, 5, 9, 16, 23 and 26. The second group received 20 mg cisplatin over 24 h commencing 1 h before each fraction of irradiation on days 1, 4, 8, 11, 15 and 18. The first series of 28 patients had 30 lesions treated. Nine (30%) of these lesions responded completely and 10 (33%) achieved partial response for an overall response rate of 63% (95% confidence interval 44–80%). Survival was not evaluated in this group. The second group was comprised of 27 patients, with one irradiated lesion each. 1 patient achieved a complete response and 13 (48%) a partial response for an overall response rate of 52% (32–71%). Median survival was 21 weeks (16–31 weeks). Treatment was well tolerated with nausea and vomiting being the most common toxicity. Synchronous cisplatin infusion with radiotherapy achieves high response rates in metastatic melanoma. Whether it is superior to radiotherapy alone will require evaluation in a randomised trial.
Eur J Cancer, Vol. 27, No. 12, pp. 1564–1566, 1991.

INTRODUCTION

RADIOTHERAPY, FREQUENTLY in large dose fractions, has been used in the palliative treatment of metastatic malignant melanoma [1]. Its efficacy may be limited by the ability of melanoma cells to repair DNA damage induced by radiotherapy [2].

In vitro animal and human studies have indicated the potential for cisplatin to act as a radiosensitiser in a variety of tumours [3, 4]. Possible mechanisms include the activity of cisplatin as an hypoxic cell sensitizer [5], an inhibitor of DNA repair [6] and as a depletor of protein bound thiols [7]. Radiosensitisation appears to be maximal when cisplatin is given prior to radiotherapy [8] although the most effective schedule for combined treatment is yet to be established [3].

Two small studies have reported high response rates using